Auxiliary material for Paper 2010TC002668

Evolution of the Adria-Europe plate boundary in the northern Dinarides: From continent-continent collision to back-arc extension

Kamil Ustaszewski
Institute of Geology and Paleontology, University of Basel, Basel, Switzerland

Now at Lithosphere Dynamics, GFZ German Research Centre for Geosciences, Potsdam, Germany

Alexandre Kounov
Institute of Geology and Paleontology, University of Basel, Basel, Switzerland

Stefan M. Schmid
Department of Earth Sciences, Freie Universitaet Berlin, Berlin, Germany

Urs Schaltegger
Department of Mineralogy, University of Geneva, Geneva, Switzerland

Erwin Krenn,
Division of Mineralogy, Department of Materials Science and Physics, University of Salzburg, Salzburg, Austria

Wolfgang Frank
Central European Argon Laboratory, Geological Institute, Slovak Academy of Sciences, Bratislava, Slovakia

Institute for Geology, University of Vienna, Vienna, Austria

Bernhard Fuegenschuh,
Geological-Paleontological Institute, Innsbruck, Austria

Ustaszewski, K., A. Kounov, S. M. Schmid, U. Schaltegger, E. Krenn, W. Frank, and B. Fuegenschuh (2010), Evolution of the Adria-Europe plate boundary in the northern Dinarides: From continent-continent collision to back-arc extension, Tectonics, 29, XXXXXX, doi:10.1029/2010TC002668.

Introduction

This data set contains supplemental descriptions of analytical techniques, figures and data sets accompanying the paper 2010TC002668. Text S1 describes analytical techniques involved in geochronological dating (section S1), details on the mineral chemistry of the dated minerals (section S2), as well as a description of the apatite fission track modeling technique (section S3). The figures and data sets are referred to in the main manuscript text.

1. 2010tc002668-txts01.doc
Analytical techniques, chemistry of minerals analyzed by 40Ar/39Ar dating, and apatite fission track thermal modeling.
1.1. Section S1: analytical techniques
    - U/Pb dating
    - 40Ar/39Ar mineral dating

- Zircon and Apatite fission-track dating
- References

1.2. Section S2: Chemistry of minerals analyzed by 40Ar/39Ar dating
1.3. Section S3: Apatite fission track thermal modeling

2. 2010tc002668-fs01.eps

Results of phase equilibrium modeling ('pseudosection modeling') for metapelitic sample UK06-62 from the Motajica Inselberg, calculated using Perple_X [Connolly, 2005; version 7]. Stable assemblages were constrained from the whole-rock composition (Data Set S2) in the system Na2O-CaO-K2O-FeO-MgO-MnO-Al2O3-SiO2-H2O-CO2 with water in excess (saturated phase). With reference to the P-T range under study and for the lack of secondary CO2-bearing phases, a water activity of 1 was assumed. No substantial changes of the garnet stability field will occur by using a water activity of 0.9. Shown in red are the garnet (GRT) and Staurolite (St) stability field. Note that the temperature axis is labeled in Kelvin. The results indicate P-T conditions between about 5 and 8 kbar and 560 to 640 degrees C for the parageneses observed in the studied sample. These results are fairly compatible with our P-T estimated described in the main manuscript. Compare with Fig. 12 in the main manuscript.

3. 2010tc002668-fs02.eps
Concordia diagrams showing the results of single zircon and monazite analyses from Prosara (a) and Motajica samples (b). Individual analyses are shown as 2Łm error ellipses. Given ages are weighted mean 206Pb/238U ages in case of zircons and 207Pb/235U ages in case of monazite. Grey shading indicates the uncertainties of the decay constants. See Figures 6 and 7 in the main manuscript for sample locations.

4. 2010tc002668-fs03.eps
Backscattered electron images of amphiboles from Motajica analyzed by the 40Ar/39Ar stepwise heating technique. Numbered points correspond to the mineral analyses in Data Set S5. See Figure 7d for location.

5. 2010tc002668-fs04.eps
Backscattered electron images of sericite aggregates analyzed by the 40Ar/39Ar stepwise heating technique. (a.) The sericite aggregates occur as mm-thin layers within a greenschist facies calcite marble from Prosara (sample UK06-58, see Figure 6a for location). The sericites define an s1 foliation, which is crenulated during the D2 deformation event. Cc = calcite, Ser = sericite, Mt = magnetite. (b.) At greater magnification, the sericite aggregates are identified as intergrowths of muscovite (Ms) and chlorite (Chl) by different shades of gray.

6. 2010tc002668-fs05.eps
Frequency distribution of the zircon single grain ages from the analyzed Maastrichtian samples from the Motajica inselberg. Also shown are the depositional age range of the Maastrichtian flysch, magmatic activities in the area and the Zr FT age obtained on a Paleozoic granite of the

Papuk-Psunj Mountain. Refer to section 5.3 in the main manuscript. See Figure 7 for sample locations.

7. 2010tc002668-ds01.doc
Compilation of biostratigraphic ages reported for the Cretaceous to Paleogene formations in the Sava Zone inselbergs, sorted from north to south.

8. 2010tc002668-ds02.doc
Bulk and mineral composition of an amphibolite facies metapelite (sample UK06-62) from Motajica used for thermobarometric calculations. See Figure 7b for sample location.

9. 2010tc002668-ds03.doc
U-Pb isotopic data of analyzed zircons and monazites from Prosara and Motajica igneous rocks.

10. 2010tc002668-ds04.doc
40Ar/39Ar analytical data for incremental heating experiments on mineral concentrates and fine fractions from Prosara and Motajica.

11. 2010tc002668-ds05.doc
Electron-microprobe analyses of amphiboles dated by the 40Ar/39Ar stepwise heating technique.

12. 2010tc002668-ds06.doc
Summary of geochronological data from the Sava Zone used for constraining its thermal evolution. The data are separated into a footwall (italics) and hangingwall unit with respect to the Motajica detachment. All data except those indicated by superscripts were derived in this study. Compare with Figure 15 in the main manuscript.

Supplementary material for electronic supplement to:
Ustaszewski K. et al., Tectonics, doi:10.1029/2010TC002668, 2010

Section S1: analytical techniques

U-Pb dating

Zircons and monazites were prepared by standard mineral separation techniques (crushing, milling, concentration via Wilfley table, magnetic separation and heavy liquid separation in methylene iodide (density > 3.1 gcm^{-3})). Suitable grains were then handpicked in ethanol under a binocular microscope. In order to minimize effects of secondary lead-loss in zircons, the chemical abrasion "CA-TIMS" technique, involving high-temperature annealing followed by a subsequent HF leaching step [*Mattinson*, 2005] was applied. The monazite preparation followed procedures described in *Schaltegger et al*. [2005]. Isotopic analyses were performed at the Department of Earth Sciences at the University of Geneva. The analytical techniques are described in *Ovtcharova et al*. [2006] in more detail. Calculation of ^{206}Pb/^{235}U ages was done with the Isoplot/Ex v.3 program [*Ludwig*, 2005].

^{40}Ar/^{39}Ar mineral dating

Mineral separation: The ^{40}Ar/^{39}Ar incremental heating technique was applied to amphibole concentrates, sericite aggregates and fine fractions, using the facilities of the Central European Argon-Laboratory (CEAL) at the Geological Institute of the Slovak Academy of Science in Bratislava. Amphibole concentrates and sericite aggregates have been prepared by standard mineral separation techniques (crushing, milling, sieving, magnetic separation and handpicking under a binocular microscope). Fine fractions in three different grain size ranges (<2, 2–6 and 6–12 μm) have been prepared from calcite marbles following decarbonation with acetic acid. Samples selected for fine fraction separation were only jaw-crushed and sieved without milling, in order to minimize the production of an additional fine fraction during preparation. Fine fractions were separated by settling from a suspension in Atterberg cylinders applying Stoke's Law. Mineral phases of all analyzed fine fractions were determined by XRD on a Siemens D5000 at the Institute of Mineralogy & Petrography of the University Basel. In order to avoid contribution of low-K phases (quartz, chlorite, kaolinite and smectite) only very illite-rich fine fractions were selected for dating. Prior to dating, amphibole chemistry was determined with emphasis on K_2O content (section S2).

Irradiation and gas extraction: Mineral concentrates were enclosed in high purity quartz vials and irradiated for 4–6 h at the 9 MW ASTRA reactor at the Austrian Research

Centre Seibersdorf. After a cooling period of at least 3 weeks, the samples were filled in annealed (low-blank) cylindrical tantalum capsules. Two Ar-extraction lines were used during this study, a manually operated and a fully automatic extraction and purification line. Argon was released at progressively higher temperatures, ranging between 590 and 1250 °C and between 750 and 1300 °C for the white mica and amphibole concentrates, respectively. During the analysis only one tantalum capsule was in the heating position. The heating time for the low temperature steps was typically 10 min and was continuously lowered to 3 min for the high temperature steps. Cleaning of the gas was done by a combination of cold traps, Ti-sponge and SAE-getters. A collection of the argon with a cold trap before sample inlet was not performed. Two thirds of the gas was introduced into a VG-5400 gas mass spectrometer; the rest was pumped away from the extraction line. Isotopic ratios were determined for a measuring period of 10 min, with the local ratios extrapolated back to the time of sample inlet to determine the original isotopic composition. Ages were calculated after corrections for mass discrimination and radioactive decay, especially of ^{37}Ar, using formulas given by *McDougall and Harrison* [1999]. The specific production ratios of the interfering Ar isotopes at the ASTRA reactor of Seibersdorf are: $(^{36}Ar/^{37}Ar)_{Ca}=0.0003$, $(^{39}Ar/^{37}Ar)_{Ca}=0.00065$, $(^{40}Ar/^{39}Ar)_{K}=0.025$. The K/Ca ratio is determined from the $^{39}Ar/^{37}Ar$ ratio (calculated for the end of irradiation) using a conversion factor of 0.247. This factor was determined from a plagioclase with uniform and well known composition.

The ^{40}Ar line blank at 1000 °C is 2–5×10−10 cm^3 STP and the $^{40}Ar/^{36}Ar$ ratio of the line blank is close to air composition. Determination of the background, blank corrections and careful checking of the peak positions were routinely performed. J-values were determined with internal laboratory standards, calibrated by international standards including muscovite Bern 4M [*Burghele*, 1987], amphibole Mm1Hb [*Samson and Alexander*, 1987] and Fish Canyon sanidine [*Renne et al.*, 1994].

Data analysis: We use the plateau age definition of *Frank and Schlager* [2006]. A plateau age is defined if three or more contiguous heating steps with similar apparent K/Ca ratios, each representing >4 % of the total ^{39}Ar released and summing up to >30 % of the total quantity of ^{39}Ar released, coincide within ±1 % analytical uncertainty. We defined a so-called 'mean age' if three or more contiguous heating steps failed the criteria of a plateau age in terms of ±1 % analytical uncertainty, but which still gave similar ages within a variance of ≤15 %. Total gas ages are calculated by integrating over all heating steps, but do not carry geological significance unless they coincide with the plateau ages within analytical uncertainties. Errors of the calculated ages for the individual steps are given as 1σ. The 1σ errors of the plateau and total gas ages include an additional error of ±0.4 % on the J-value.

The contribution of low-K phase impurities to the released ^{39}Ar was evaluated by inspecting the K/Ca ratio. Loss of ^{39}Ar through the recoil effect is quoted to often severely restrict the applicability of the $^{40}Ar/^{39}Ar$ dating technique in clay-size fractions [e.g. *Turner and Cadogan*, 1974; *Faure*, 1986; *McDougall and Harrison*, 1999]. However, *Dong et al.* [1995; 1997a, b] demonstrated how vacuum encapsulation prior to irradiation mitigated this effect, yielding geologically meaningful ages even on <2 μm fractions. *Frank and Schlager* [2006] also successfully demonstrated the applicability of this technique on small grain size fractions. We consider this technique a viable approach for dating fine fractions from sub-greenschist-facies and greenschist-facies pelites.

Zircon and Apatite fission-track dating

Whole rock samples were crushed and apatite and zircon grains were recovered by conventional heavy liquid and magnetic methods. Apatite grains were mounted in epoxy resin, polished and etched with 7% HNO_3 at 21 °C for 50 s. Zircon grains were etched in an eutectic mixture of KOH and NaOH at 220 °C for between 9 and 15 h. Irradiation was carried out at the OSU facility, Oregon State University Radiation Center, USA. Microscopic analysis was completed at Basel University using an optical microscope with a Kinetek computer-driven stage [*Dumitru*, 1995]. All ages were determined using the z approach [*Hurford and Green*, 1983] with a z value of 332±7 for apatite (CN5 standard glass) and 122±2 for zircon (CN1 standard glass) (Table 1, analyst: A. Kounov). They are reported as central ages [*Galbraith and Laslett*, 1993] with a 2σ error (Table 1). The magnification used was x1250 for apatite and x1600 (dry objective) for zircon. Horizontal confined track lengths in apatite grains were measured at a magnification of x1250. Fission track etch pit diameters (Dpar) were measured at a magnification of x2500 in order to estimate the compositional influence on fission track annealing [*Carlson et al*., 1999].

The temperatures at which fission tracks in apatite and zircon minerals partially anneal (i.e. partial isotopic resetting) are not sharply defined. A temperature range, known as partial annealing zone (PAZ), exists where partial track annealing occurs. The effective closure of the system lies within this zone and is dependent on the overall cooling rates and the kinetic properties of the minerals. The specific partial annealing zone for apatite lies between 60 °C and 110 °C [*Green and Duddy*, 1989; *Corrigan*, 1993], with one mean effective closure temperature constrained at 110±10 °C.

Unfortunately our knowledge of zircon annealing is not as advanced as that of apatite and wide-ranging values for the temperature bounds for the partial annealing zone of zircon have been published. *Yamada et al*. [1995] suggest temperature limits of ~390–170 °C, whereas *Tagami and Dumitru* [1996] and *Tagami et al*. [1998] suggested temperature limits of ~310–230 °C. Recently in his overview on the zircon fission track dating method *Tagami* [2005] reported temperature ranges for the closure temperature between ~300–200 °C. Accordingly we use a value of 250±50 °C for closure temperature with a partial annealing zone from 200 to 300 °C.

Section S2: Chemistry of minerals analyzed by $^{40}Ar/^{39}Ar$ dating

Amphiboles: The analyses were performed by Jürgen Konzett on a JEOL microprobe at the Institute of Mineralogy & Petrography at the University Innsbruck. Amphiboles from sample M120a show prograde-zoned Ca-amphiboles with greenschist-facies actinolithic cores (poor in Al, Na and Ti) and amphibolite-facies (Al-Na-Ti-rich) rims of Mg-hornblende (Figure S3a and b in the electronic supplement). Except for the Al-poor cores, all amphiboles have K_2O contents between 0.3 and 0.4 wt% (Data Set S5). Amphiboles in sample M129 show K_2O contents between c. 0.1 and 0.3 wt%. Sample M129 also shows strongly zoned Ca-amphiboles and, in addition, Fe-Mg-amphiboles (likely Cummingtonit). The latter occur as irregular inclusions and exsolution lamellae that appear brighter than the host mineral (Figure S3c). This suggests a coexistence of Ca- and Mg-Fe amphiboles rather than a mineral reaction.

Sericites: Sericites from sample UK06-58 (Figure S4 in the electronic supplement) dated in this study were analyzed in-situ within the calcite marbles by back-scattered electrons and energy-dispersive chemical analyses on a scanning electron microscope at GFZ Potsdam with the help of Helga Kemnitz. Detailed chemical analyses are available from the first author upon request.

Section S3: Apatite fission track thermal modeling

Fission tracks in apatites are formed continuously through time at an approximately uniform initial mean length of ~16.3 μm [*Gleadow et al.*, 1986]. Upon heating, tracks gradually anneal and shorten to a length that is function of the time and maximum temperature to which the apatites were exposed. For example, tracks are completely annealed at a temperature of 110 - 120 °C for a period of 10^5 - 10^6 years [*Gleadow and Duddy*, 1981]. These annealing characteristics allow the generation of time-temperature paths by inverse modeling [e.g. *Gallagher*, 1995; *Ketcham et al.*, 2000]. As resolution of the AFT thermochronometer is limited to the temperature range of 60-110 °C [*Laslett et al.*, 1987], therefore the paths of the t-T envelope defined for the zones out of this range are not necessary representative for the real thermal evolution of a sample.

Modeling of the apatite age and track length distribution data was carried out with the program HeFTy [*Ketcham et al.*, 2000]. FT age, track-length distribution and etch pits diameters (Dpar) as well as user-defined time (t) - temperature (T) boxes, are used as input parameters. An inverse Monte Carlo algorithm with multikinetic annealing model [*Ketcham et al.*, 2007] was used to generate the time-temperature paths. The algorithm generates a large number of time-temperature paths, which are tested with respect to input data. The t-T paths are forced to pass through the time-temperature boxes (constraints). The fitting of the measured input data and modeled output data is statistically evaluated and characterized by value of the goodness of fit (GOF). A "good" result corresponds to value >0.5 whereas value of 0.05 or higher is considered to reflect an "acceptable" fit between modeled and measured data.

It is important to remember that the best thermal history obtained during this process is not necessarily the only possible. Other thermal histories may match the observed data similarly well and it is therefore imperative to consider as many other geological constraints as possible to determine the most likely path.

References

Burghele, A. (1987), Propagation of error and choice of standard in the ^{40}Ar–^{39}Ar technique, *Chemical Geology*, *66*, 17-19.

Carlson, D. W., R. A. Donelick, and R. A. Ketcham (1999), Variability of apatite fission-track annealing kinetics, I. Experimental results, *American Mineralogist*, *84*, 1213-1223.

Corrigan, J. D. (1993), Apatite fission-track analysis of Oligocene strata in South Texas, U.S.A.: Testing annealing models, *Chemical Geology*, *104*, 227-249.

Dong, H., C. M. Hall, and A. N. Halliday (1995), Mechanisms of argon retention in clays revealed by laser ^{40}Ar-^{39}Ar dating, *Science*, *267*, 355-359.

Dong, H., C. M. Hall, A. N. Halliday, and D. R. Peacor (1997a), Laser ^{40}Ar-^{39}Ar dating of microgram-size illite samples and implications for thin section dating, *Geochimica et Cosmochimica Acta*, *61*, 3803-3808.

Dong, H., C. M. Hall, A. N. Halliday, D. R. Peacor, R. J. Merriman, and B. Roberts (1997b), ^{40}Ar-^{39}Ar illite dating of Late Caledonian (Acadian) metamorphism and cooling of K-bentonites and slates from the Welsh Basin, U.K., *Earth and Planetary Science Letters*, *150*, 337-351.

Dumitru, T. A. (1995), A new computer automated microscope stage system for fission track analysis, *Nuclear Tracks Radiation Measurements*, *21*, 575-580.

Faure, G. (1986), *Principles of Isotope Geology*, 2nd ed., 589 pp., John Wiley & Sons, New York.

Frank, W., and W. Schlager (2006), Jurassic strike slip versus subduction in the Eastern Alps, *International Journal of Earth Sciences*, *95*, 431-450.

Galbraith, R. F., and G. M. Laslett (1993), Statistical models for mixed fission-track ages, *Nuclear Tracks and Radiation Measurements*, *21*, 459-470.

Gallagher, K. (1995), Evolving temperature histories from apatite fission-track data, *Earth and Planetary Sciences Letters*, *136*, 421-435.

Gleadow, A. J. W., I. R. Duddy, P. F. Green, and K. A. Hegarty (1986), Fission track length in the apatite annealing zone and interpretation of mixed ages, *Earth and planetary Science Letters*, *78*, 245-254.

Gleadow, A. J. W., and I. R. Duddy (1981), A natural long-term track annealing experiment for apatite, *Nuclear Tracks and Radiation Measurements*, *5*, 169–174.

Green, P. F., and I. R. Duddy (1989), Some comments on paleotemperature estimation from apatite fission track analysis, *Journal of Petroleum Geology*, *12*, 111-114.

Hurford, A. J., and P. F. Green (1983), The zeta age calibration of fission-track dating, *Chemical Geology*, *41*, 285-317.

Ketcham, R., R. A. Donelick, and M. Donelick (2000), AFTSolve: A program for multi-kinetic modeling of apatite fission-track data, *Geological Materials Research*, *1*, 1-32.

Ketcham, R. A., A. Carter, R. A. Donelick, J. Jocelyn Barbarand, and A. J. Hurford (2007), Improved modeling of fission-track annealing in apatite, *American Mineralogist*, *92*, 799-810.

Laslett, G. M., P. F. Green, I. R. Duddy, and A. J. W. Gleadow (1987), Thermal annealing of fission track in apatite, 2. A quantitative analysis, *Chemical Geology*, *65*, 1-13.

Ludwig, K. (2005), Isoplot - A plotting and regression program for radiogenic isotope data, in *USGS Open File report 91-445*, edited, Boulder.

Mattinson, J. M. (2005), Zircon U-Pb chemical abrasion ("CA-TIMS") method: Combined annealing and multi-step partial dissolution analysis for improved precision and accuracy of zircon ages, *Chemical Geology*, *220*, 47-66.

McDougall, I., and T. M. Harrison (1999), *Geochronology and Thermochronology by the* $^{40}Ar/^{39}Ar$ *method*, 2nd ed., 269 pp., Oxford University Press, New York.

Ovtcharova, M., H. Bucher, U. Schaltegger, T. Galfetti, A. Brayard, and J. Guex (2006), New Early to Middle Triassic U-Pb ages from South China: Calibration with ammonoid biochronozones and implications for the timing of the Triassic biotic recovery, *Earth and Planetary Science Letters*, *243*, 463-475.

Renne, P. R., A. L. Deino, R. C. Walter, B. D. Turrin, C. C. Swisher, T. A. Becker, G. H. Curtis, W. D. Sharp, and A. R. Jaouni (1994), Intercalibration of astronomical and radioisotopic time, *Geology*, *22*, 783-786.

Samson, S. D., and E. C. Alexander (1987), Calibration of the interlaboratory ^{40}Ar–^{39}Ar dating standard MMhb-1, *Chemical Geology*, *66*, 27-34.

Schaltegger, U., T. Pettke, A. Audétat, E. Reusser, and C. A. Heinrich (2005), Magmatic-to-hydrothermal crystallization in the W–Sn mineralized Mole Granite (NSW, Australia) Part I: Crystallization of zircon and REE-phosphates over three million years—a geochemical and U–Pb geochronological study, *Chemical Geology*, *220*, 215– 235.

Stacey, J. S., and J. D. Kramers (1975), Approximation of terrestrial lead isotope evolution by a two-stage model, *Earth and Planetary Science Letters*, *26*, 207-221.

Tagami, T. (2005) Zircon Fission-Track Thermochronology and Applications to Fault Studies, *Reviews in Mineralogy and Geochemistry*, *58*, 95-122.

Tagami, T., and T. A. Dumitru (1996), Provenance and history of the Franciscan accretionary complex: Constraints from zircon fission track thermochronology, *Journal of Geophysical Research*, *101*, 8345-8255.

Tagami, T., R. F. Galbraith, R. Yamada, and G. M. Laslett (1998), Revised annealing kinetics of fission tracks in zircon and geological implications, in *Advances in Fission-Track Geochronology* edited by P. Van den Haute and F. de Corte, pp. 99-114, Kluwer Academic Publishers, Dordrecht.

Turner, G., and P. H. Cadogan (1974), Possible effects of ^{39}Ar recoil in ^{40}Ar-^{39}Ar dating, *Geochimica et Cosmochimica Acta*, *2, Supplement 5*, 1601-1615.

Yamada, R., T. Tagami, S. Nishimura, and H. Ito (1995), Annealing kinetics of fission tracks in zircon: an experimental study, *Chemical Geology*, *122*, 249-248.

Figures for electronic supplement

Figure S1: Results of phase equilibrium modeling ('pseudosection modeling') for metapelitic sample UK06-62 from the Motajica Inselberg, calculated using Perple_X [*Connolly*, 2005; version 7]. Stable assemblages were constrained from the whole-rock composition (Data Set S2) in the system Na2O–CaO–K2O–FeO–MgO–MnO–Al2O3–SiO2–H2O–CO2 with water in excess (saturated phase). With reference to the P-T range under study and for the lack of secondary CO2-bearing phases, a water activity of 1 was assumed. No substantial changes of the garnet stability field will occur by using a water activity of 0.9. Shown in red are the garnet (GRT) and Staurolite (St) stability field. Note that the temperature axis is labeled in Kelvin. The results indicate P-T conditions between about 5 and 8 kbar and 560 to 640 °C for the parageneses observed in the studied sample. These results are fairly compatible with our P-T estimated described in the main manuscript. Compare with Fig. 12 in the main manuscript.

Figure S2: Concordia diagrams showing the results of single zircon and monazite analyses from Prosara (a) and Motajica samples (b). Individual analyses are shown as 2σ error ellipses. Given ages are weighted mean $^{206}Pb/^{238}U$ ages in case of zircons and $^{207}Pb/^{235}U$ ages in case of monazite. Grey shading indicates the uncertainties of the decay constants. See Figures 6 and 7 in the main manuscript for sample locations.

Figure S3: Back-scattered electron images of amphiboles from Motajica analyzed by the $^{40}Ar/^{39}Ar$ stepwise heating technique. Numbered points correspond to the mineral analyses in Data Set S5. See Figure 7d in the main manuscript for location.

Figure S4: Back-scattered electron images of sericite aggregates analyzed by the $^{40}Ar/^{39}Ar$ stepwise heating technique. (a.) The sericite aggregates occur as mm-thin layers within a greenschist-facies calcite marble from Prosara (sample UK06-58, see Figure 6a for location). The sericites define an s1 foliation, which is crenulated during the D2 deformation event. Cc = calcite, Ser = sericite, Mt = magnetite. (b.) At greater magnification, the sericite aggregates are identified as intergrowths of muscovite (Ms) and chlorite (Chl) by different shades of gray.

Figure S5: Frequency distribution of the zircon single grain ages from the analyzed

Maastrichtian samples from the Motajica inselberg. Also shown are the depositional age range of the Maastrichtian flysch, magmatic activities in the area and the Zr FT age obtained on a Palaeozoic granite of the Papuk-Psunj Mountain. Refer to section 5.3 in the main manuscript. See Figure 7 in the main manuscript for sample locations.

Data Sets for electronic supplement

Data Set S1: Compilation of biostratigraphic ages reported for the Cretaceous to Palaeogene formations in the Sava Zone inselbergs, sorted from north to south.

Data Set S2: Bulk and mineral composition of an amphibolite-facies metapelite (sample UK06-62) from Motajica used for thermobarometric calculations. See Figure 7b for sample location.

Data Set S3: U-Pb isotopic data of analyzed zircons and monazites from Prosara and Motajica igneous rocks.

Data Set S4: $^{40}Ar/^{39}Ar$ analytical data for incremental heating experiments on mineral concentrates and fine fractions from Prosara and Motajica.

Data Set S5: Electron-microprobe analyses of amphiboles dated by the $^{40}Ar/^{39}Ar$ stepwise heating technique.

Data Set S6: Summary of geochronological data from the Sava Zone used for constraining its thermal evolution. The data are separated into a footwall (*italics*) and hangingwall unit with respect to the Motajica detachment. All data except those indicated by superscripts were derived in this study. Compare with Figure 15 in the main manuscript.

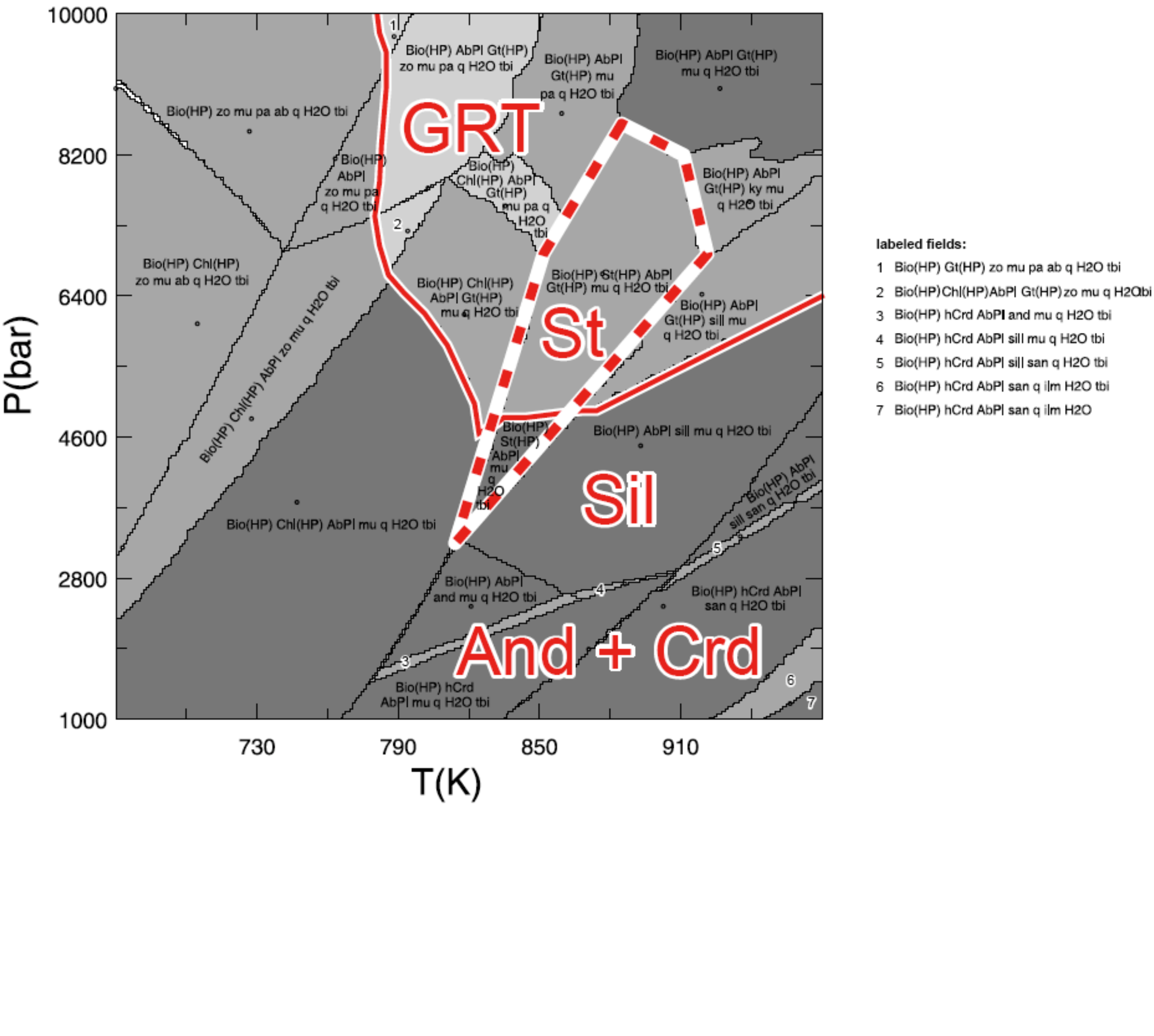

10000
8200
6400
4600
2800
1000
P(bar)
730
790
850
910
T(K)
GRT
St
Sil
And + Crd
Bio(HP) AbPl Gt(HP) zo mu pa q H2O tbi
Bio(HP) AbPl Gt(HP) mu pa q H2O tbi
Bio(HP) AbPl Gt(HP) mu q H2O tbi
Bio(HP) zo mu pa ab q H2O tbi
Bio(HP) AbPl zo mu pa q H2O tbi
Bio(HP) Chl(HP) AbPl Gt(HP) mu pa q H2O tbi
Bio(HP) AbPl Gt(HP) ky mu q H2O tbi
Bio(HP) Chl(HP) zo mu ab q H2O tbi
Bio(HP) Chl(HP) AbPl Gt(HP) mu q H2O tbi
Bio(HP) St(HP) AbPl Gt(HP) mu q H2O tbi
Bio(HP) AbPl Gt(HP) sill mu q H2O tbi
Bio(HP) Chl(HP) AbPl zo mu q H2O tbi
Bio(HP) St(HP) AbPl mu q H2O tbi
Bio(HP) AbPl sill mu q H2O tbi
Bio(HP) Chl(HP) AbPl mu q H2O tbi
Bio(HP) AbPl sill san q H2O tbi
Bio(HP) AbPl and mu q H2O tbi
Bio(HP) hCrd AbPl san q H2O tbi
Bio(HP) hCrd AbPl mu q H2O tbi
labeled fields:
1 Bio(HP) Gt(HP) zo mu pa ab q H2O tbi
2 Bio(HP) Chl(HP) AbPl Gt(HP) zo mu q H2O tbi
3 Bio(HP) hCrd AbPl and mu q H2O tbi
4 Bio(HP) hCrd AbPl sill mu q H2O tbi
5 Bio(HP) hCrd AbPl sill san q H2O tbi
6 Bio(HP) hCrd AbPl san q ilm H2O tbi
7 Bio(HP) hCrd AbPl san q ilm H2O

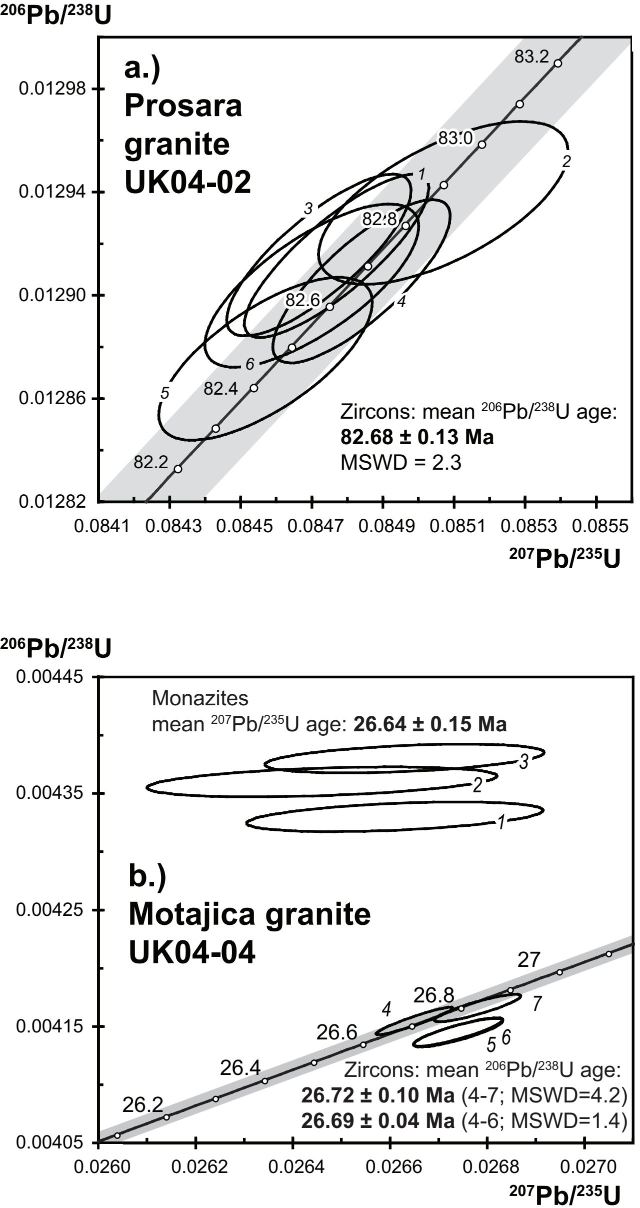

206Pb/238U
a.)
Prosara granite UK04-02
Zircons: mean 206Pb/238U age:
82.68 ± 0.13 Ma
MSWD = 2.3
207Pb/235U
206Pb/238U
Monazites
mean 207Pb/235U age: 26.64 ± 0.15 Ma
b.)
Motajica granite UK04-04
Zircons: mean 206Pb/238U age:
26.72 ± 0.10 Ma (4-7; MSWD=4.2)
26.69 ± 0.04 Ma (4-6; MSWD=1.4)
207Pb/235U

Fig. S2

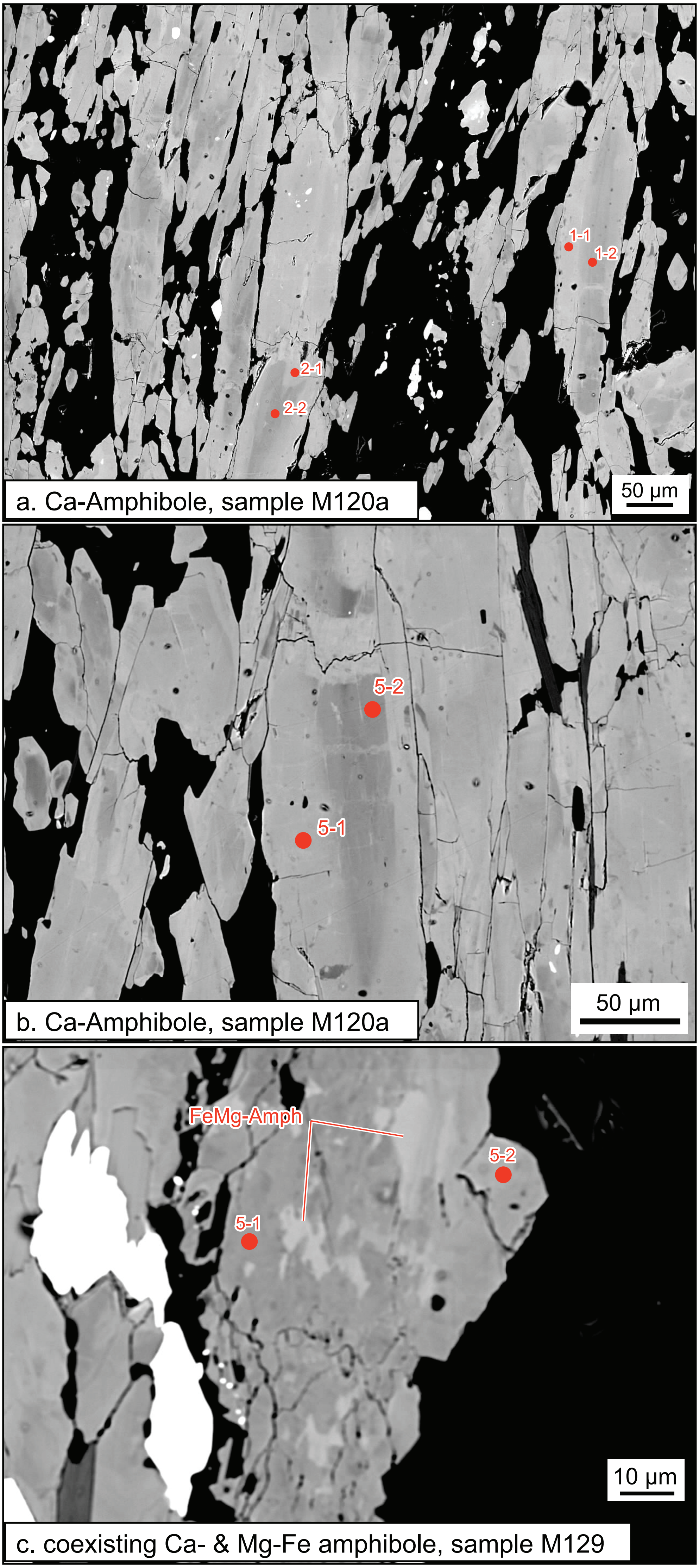
1-1
1-2
2-1
2-2
50 µm
a. Ca-Amphibole, sample M120a
5-2
5-1
50 µm
b. Ca-Amphibole, sample M120a
FeMg-Amph
5-2
5-1
10 µm
c. coexisting Ca- & Mg-Fe amphibole, sample M129

Fig. S3

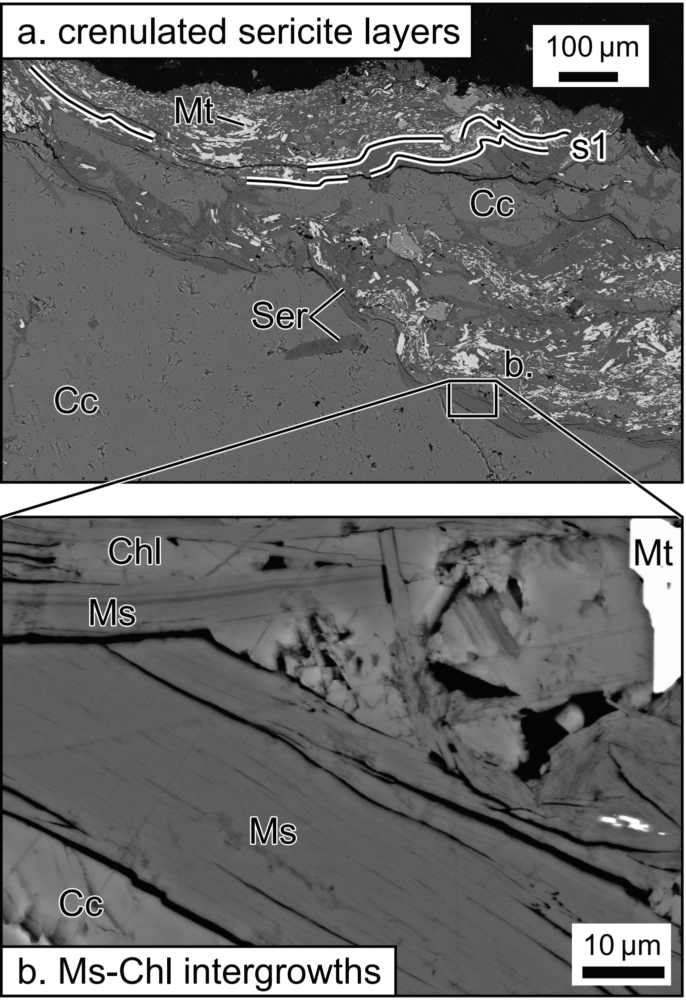
a. crenulated sericite layers
100 μm
Mt
s1
Cc
Ser
b.
Cc
Chl
Mt
Ms
Ms
Cc
10 μm
b. Ms-Chl intergrowths

Fig. S4

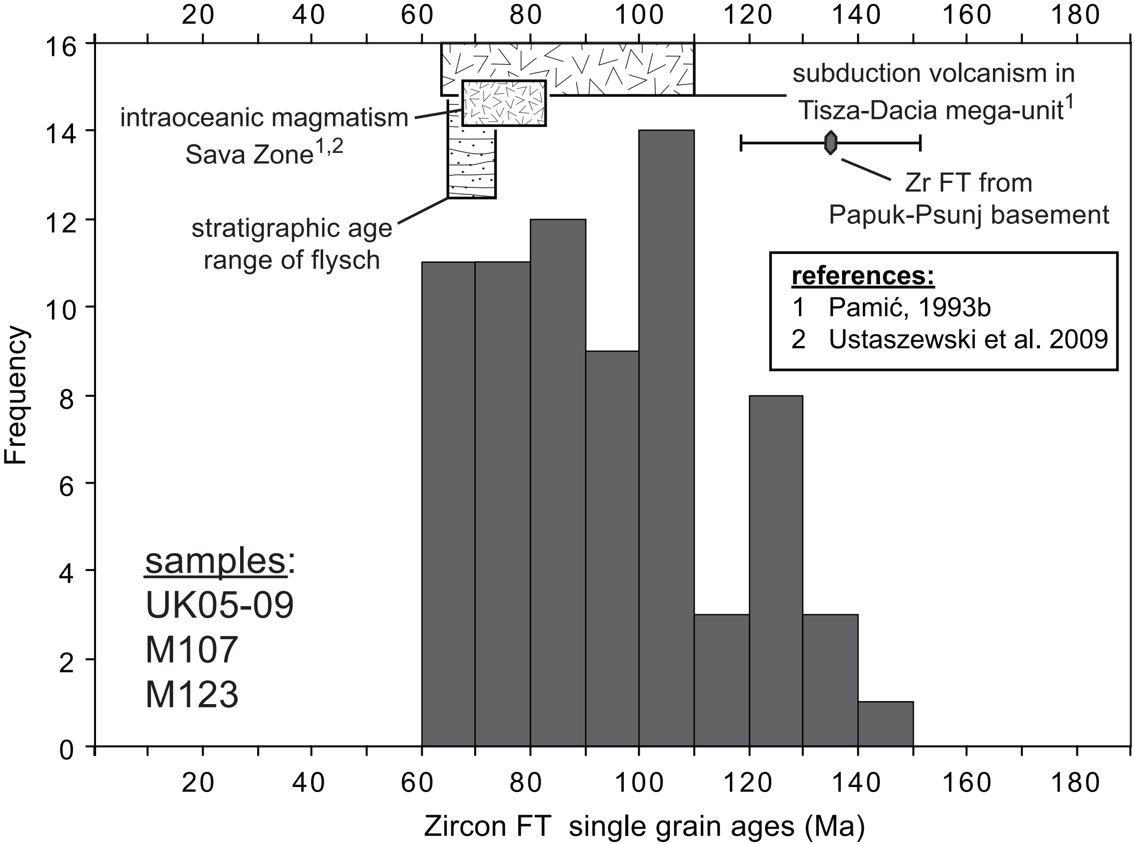

subduction volcanism in
Tisza-Dacia mega-unit[1]
intraoceanic magmatism
Sava Zone[1,2]
stratigraphic age
range of flysch
Zr FT from
Papuk-Psunj basement
references:
1 Pamić, 1993b
2 Ustaszewski et al. 2009
samples:
UK05-09
M107
M123
Frequency
Zircon FT single grain ages (Ma)

Fig. S5

Data Set S1: Compilation of biostratigraphic ages reported for Cretaceous to Paleogene formations in the Sava Zone

inselberg	**map sheet**[1]	**mapped lithology**[2, 3]	**Locality**[4]	**Lithology**[5]	**fossils**	**Age assignment**	**Reference**[6]
Požeška Gora	Nova Kapela	"K2, 2+3"	Vrbovac Topolika Bukovac	Marls Marly limestones Sandstones Calcarenites conglomerates	*Globotruncana lapparenti* *Globotruncana stuarti* *G. area* *G. cf. convexa*	Turon-Senon	Šparica et al., 1980
Požeška Gora	Nova Kapela	?"K2, 2+3"	Nakop potok creek	limestones	*Globotruncana lapparenti lapparenti (*Brotzen*)* *Globotruncana lapparenti tricarinata (*Quereau*)* *Globotruncana stuarti (*De Lapparent*)* *Globotruncana arca (*Cushman*)* *Globotruncana lapparenti bulloides* *Gl. sp. (*cf. *fornicata* Plummer*)* *Praeglobotruncana citae (*Bolli*)* *Heterohelicidae* *Globigerinidae (?)*	"Upper Cretaceous, upper parts of the Senonian" **= Late Campanian – Maastrichtian**	Šparica et al., 1980 Pamić & Šparica 1983 M. Caron, pers. comm. July 2007
Prosara	Nova Gradiska	"GK2,3" "SmK2,3" "SqmK2,3" "ArK2,3"		Phyllites meta-arcoses sandstones micaschists Qu-schists argillo-schists	palynomorphs	Maastricht - Lower Paleocene	Šparica et al., 1984
Prosara	Kostajnica	"GK2,3" "SqmK2,3" "ArK2,3"		phyllites	microflora	Upper Cretaceous - Lower Paleocene	Jovanović and Magas, 1986
Motajica	Nova Kapela	"FK2,3" (and "ArK2,3"?)	Gladalica creek	argillo-phyllites metasandstones	palynomorphs: angiosperm pollen (conifers?)	Uppermost Cretaceous - Lowermost Palaeogene	Pantic and Jovanović, 1970

Data Set S1: Compilation of biostratigraphic ages reported for Cretaceous to Paleogene formations in the Sava Zone

inselberg	**map sheet**[1]	**mapped lithology**[2, 3]	**Locality**[4]	**Lithology**[5]	**fossils**	**Age assignment**	**Reference**[6]
Motajica	Nova Kapela	"FK2,3" "ArK2,3"		Arcoses phyllites	angiosperm pollen *Siderolites calcitropoides* *Orbitoides sp.* *Rotaliidae* *Clypeorbis mamillata* rudist fragments globotruncanae	Maastricht	Šparica et al., 1980
Motajica	Nova Kapela	"4K2,3"	Sitnes, Orljak	Sandstones Clays Argillites limestones, conglomerates	*Orbitoides media* *Haplophragmoides sp.*	Upper Cretaceous	Šparica et al., 1980
Kozara	Kostajnica	"Pc, E"	W of Mrakovica	"Discocyclinae limestones": limestone, shales, biogenic limestones brecciated limestones	*Lithotamnium sp.* *Lithophyllum sp.* *Distichoplax biserialis* *Nummulites sp.* *Globorotaliae* *Planorbulinae* *Globigerina pseudobuloides*	Paleocene - Lower Eocene Upper Paleocene (Thanetian)	Jovanović and Magas, 1986 Ustaszewski et al., 2009
Kozara	Kostajnica	"E1,2"		"Kozara Flysch":	microflora	Lower - Mid Eocene	Jovanović and Magas, 1986
Kozara	Nova Gradiska	"E1,2"	Turjak creek	"Kozara Flysch": sandstone arcose, subarcose siltstone, shales conglomerates	*Discocyclina seunesi* *Miliolidae* *Nummulites sp.* *Lithotamnium sp.* *Rotaliidae* *Alveolina sp.* *Codiacea* *Coralinacea* *Operculina* Microflora	Lower - Mid Eocene	Šparica et al., 1984

Notes:

1) Names of map sheets correspond to the originally assigned names of the 1:100.000 map sheets of the Basic Geological Map of Former Yugoslavia, Federal Geologic Institute, Beograd.

2) The lithological code reported here corresponds to the originally assigned codes on the 1:100.000 map sheets of Former Yugoslavia

3) Note that the Campanian-age pelagic limestones on top of the Campanian magmatics in Kozara and Prosara remained unidentified in the original 1:100,000 map sheets.

4) Left blank where no particular locality was indicated in the original source

5) The dominant lithology as inferred from the distribution on the 1:100.000 geological map sheets is underlined

6) References refer to the main manuscript.

This compilation relies on the original information provided with the explanatory notes to the 1:100,000 map sheets of the Basic Geological Map of Former Yugoslavia unless indicated otherwise. The original texts were written in Serbo-Croatian (with the exception of Ustaszewski et al., 2009). Translation: K. Ustaszewski.

Data Set S2: Bulk and mineral composition of an amphibolite facies metapelite (sample UK06-62) from the Motajica inselberg used for thermobarometric calculations. See Fig. 7b for sample location.

	bulk	Ms*	*std*	Bt*	*std*	Pl*	*std*
	wt%	wt%	2σ	wt%	2σ	wt%	2σ
SiO2	67.67	46.29	*0.75*	35.96	*0.47*	64.68	*0.72*
TiO2	0.84	0.54	*0.13*	1.64	*0.36*	0.00	*0.00*
Al2O3	15.12	34.84	*0.57*	17.95	*0.41*	22.16	*0.76*
CaO	1.62	-	-	0.02	*0.02*	4.01	*0.36*
FeO	4.97	3.16	*0.25*	22.08	*0.59*	-	-
MgO	2.34	0.63	*0.08*	7.99	*0.48*	-	-
MnO	0.04	0.04	*0.02*	0.31	*0.12*	-	-
K2O	3.29	10.03	*0.20*	9.22	*0.15*	-	-
Na2O	2.05	0.74	*0.08*	0.13	*0.07*	9.74	*0.34*
Total	100.16**	96.27		95.30		100.59	

* average of 10 analyses
** inclusive loss on ignition (LOI) of 2.21%
std standard deviation
wt% weight percent

Data Set S3: U-Pb isotopic data of analyzed zircons and monazites from Prosara and Motajica igneous rocks.

Number	Weight	Concentrations				Atomic ratios							Apparent ages			Error
a)	[mg]	U [ppm]	Pb rad. [ppm]	Pb nonrad. [pg]	Th/U b)	206/204 c)	207/235 d)	Error 2σ [%]	206/238 d)	Error 2σ [%]	207/206 d)	Error 2σ [%]	206/238	207/235	207/206	corr.
Alkalifeldspar granite, Prosara UK04-2																
1 zir	0.0025	884	11.46	0.50	0.38	3739	0.08477	0.25	0.01292	0.20	0.04760	0.14	82.72	82.62	79.46	0.83
2 zir	0.0023	1112	13.94	4.78	0.25	463	0.08507	0.34	0.01294	0.20	0.04770	0.26	82.85	82.90	84.38	0.63
3 zir	0.0025	862	19.32	0.62	0.30	2959	0.08472	0.25	0.01292	0.20	0.04757	0.15	82.73	82.57	77.97	0.80
4 zir	0.0025	1473	18.91	0.69	0.34	4534	0.08484	0.24	0.01291	0.20	0.04762	0.13	82.66	82.69	80.43	0.80
5 zir	0.0020	875	11.20	0.89	0.34	1665	0.08457	0.29	0.01288	0.20	0.04764	0.21	82.47	82.43	81.40	0.69
6 zir	0.0027	695	9.91	0.63	0.74	2529	0.08470	0.29	0.01290	0.20	0.04761	0.20	82.65	82.55	79.91	0.73
Motaijca Granite, UK04-4																
1 mon	0.0015	1072	52.14	3.75	38.81	138	0.02661	0.94	0.00433	0.24	0.04457	0.86	27.86	26.67	--	0.43
2 mon	0.0016	1465	62.14	9.30	33.57	89	0.02646	1.11	0.00436	0.24	0.04399	1.04	28.06	26.52	--	0.39
3 mon	0.0029	1040	50.43	8.15	38.59	123	0.02663	0.88	0.00438	0.23	0.04409	0.81	28.18	26.69	--	0.42
4 zir	0.0132	1498	6.45	0.54	0.51	10050	0.02665	0.24	0.00415	0.23	0.04652	0.08	26.73	26.71	24.75	0.94
5 zir	0.0046	2213	9.57	0.53	0.52	5239	0.02674	0.28	0.00414	0.24	0.04679	0.15	26.66	26.79	38.60	0.84
6 zir	0.0010	6008	25.05	0.43	0.39	3877	0.02674	0.28	0.00415	0.24	0.04679	0.14	26.67	26.79	38.26	0.87
7 zir	0.0014	5401	21.68	0.48	0.25	4382	0.02678	0.27	0.00417	0.23	0.04662	0.13	26.80	26.83	30.02	0.88

a) mon=monazite, zir=zircon All zircons are annealed-leached [*Mattinson*, 2005]
b) Calculated on the basis of radiogenic Pb^{208}/Pb^{206} ratios, assuming concordancy
c) Corrected for fractionation and spike
d) Corrected for fractionation, spike, blank and common lead [*Stacey and Kramers*, 1975]

Data Set S4: $^{40}Ar/^{39}Ar$ analytical data for incremental heating experiments on various mineral concentrates and fine fractions

Prosara, sample UK06-58, fine fraction 6 - 12 µm, 15 mg **Measurement number: 4572**

Step	T[ºC]	^{39}Ar (%)[b]	^{40}Ar (mV)	rad (%)	$^{39}Ar/^{37}Ar$	$(^{36}Ar)_{Ca}$ (%)	$^{40}Ar^*/^{39}Ar$	error (± %)	age (Ma)	err. (± Ma)[c]
1	590	8.9%	29.06	95.6%	1.945	37.66%	2.02	1.06	49.7	0.52
2	620	9.8%	29.32	96.1%	3.969	28.97%	1.86	0.94	45.8	0.43
3	645	11.0%	25.96	80.7%	4.839	4.89%	1.46	1.47	36.0	0.52
4[a]	670	8.1%	13.84	71.7%	7.531	2.65%	1.06	3.17	26.3	0.83
5[a]	710	12.6%	19.04	75.0%	8.926	3.06%	0.94	3.11	23.2	0.72
6[a]	760	19.1%	30.41	82.9%	11.320	3.86%	0.99	2.02	24.4	0.49
7[a]	860	13.5%	22.30	76.8%	5.855	4.63%	1.02	3.06	25.3	0.77
8	1250	17.1%	35.58	85.9%	1.445	23.17%	1.29	1.51	31.8	0.47
							total gas age:		**31.4**	**1.13**
		cumulative ^{39}Ar defining mean age:			**53.2%**		**mean age:**		**24.7**	**1.23**

correcting factors Daly/HF = 1.00 ± 5.0% Ca 36/37 = 0.00027 K 40/39 = 0.0254

Ca 39/37 = 0.00039 J = 0.013815 ± 0.4%

Prosara, sample UK06-58, coarse-grained sericite aggregate, 90.7 mg **Measurement number: 4577**

Step	T[ºC]	^{39}Ar (%)[b]	^{40}Ar (mV)	rad (%)	$^{39}Ar/^{37}Ar$	$(^{36}Ar)_{Ca}$ (%)	$^{40}Ar^*/^{39}Ar$	error (± %)	age (Ma)	err. (± Ma)[c]
1	590	11.1%	17.78	92.6%	1.181	52.38%	1.00	2.12	24.8	0.52
2	615	9.2%	16.57	95.2%	1.630	58.41%	1.13	1.92	27.9	0.53
3	650	5.2%	10.07	91.3%	2.268	26.10%	1.20	2.55	29.7	0.75
4	680	5.4%	9.72	86.6%	2.092	18.88%	1.12	3.42	27.7	0.94
5	710	5.8%	9.97	86.3%	2.196	18.34%	1.07	1.71	26.6	0.45
6[a]	740	5.4%	8.73	79.7%	2.111	12.90%	1.00	7.64	24.8	1.89
7[a]	770	6.6%	10.55	85.6%	2.049	19.57%	1.00	2.42	24.9	0.60
8[a]	820	6.1%	9.80	86.6%	1.989	21.69%	1.00	4.51	24.8	1.11
9[a]	870	6.1%	9.92	89.3%	1.743	29.81%	1.02	2.05	25.3	0.51
10[a]	930	7.6%	12.35	85.9%	1.596	24.12%	1.01	3.92	25.1	0.98
11	1020	9.1%	15.87	90.7%	1.361	38.03%	1.08	1.62	26.8	0.43
12	1250	22.4%	39.55	91.1%	1.036	45.63%	1.10	1.71	27.2	0.46
							total gas age:		**26.4**	**1.08**
		cumulative ^{39}Ar defining plateau age:			**31.7%**		**plateau age:**		**25.0**	**1.45**

correcting factors Daly/HF = 9.20 ± 5.0% Ca 36/37 = 0.00024 K 40/39 = 0.0254

Ca 39/37 = 0.00039 J = 0.013830 ± 0.2%

Motajica, sample M120a; amphiboles, 39.4 mg **Measurement number: 4644**

Step	T[ºC]	^{39}Ar (%)[b]	^{40}Ar (mV)	rad (%)	$^{39}Ar/^{37}Ar$	$(^{36}Ar)_{Ca}$ (%)	$^{40}Ar^*/^{39}Ar$	error (± %)	age (Ma)	err. (± Ma)[c]
1	750	1.8%	4.90	70.3%	0.387	3.65%	12.08	6.11	269.8	15.32
2	850	2.5%	2.43	76.4%	0.220	20.71%	4.23	5.33	99.1	5.14
3[a]	950	7.9%	4.62	89.8%	0.121	68.38%	2.54	5.61	60.2	3.32
4[a]	1000	13.6%	7.57	70.3%	0.083	47.02%	2.42	6.69	57.5	3.79
5[a]	1025	41.8%	23.77	91.5%	0.081	80.08%	2.48	2.81	58.8	1.63
6[a]	1050	3.0%	1.68	97.3%	0.084	93.10%	2.46	5.69	58.4	3.27
7[a]	1200	2.1%	1.11	96.6%	0.073	92.62%	2.35	7.06	55.8	3.88
8[a]	1350	27.3%	15.36	75.3%	0.058	61.61%	2.46	5.15	58.3	2.95
							total gas age:		**63.3**	**6.65**
		cumulative ^{39}Ar defining plateau age:			**95.7%**		**plateau age:**		**58.5**	**6.00**

correcting factors Daly/HF = 8.41 ± 5.0% Ca 36/37 = 0.00025 K 40/39 = 0.00254

Ca 39/37 = 0.00039 J = 0.013352 ± 0.4%

Motajica, sample M129; amphiboles, 23.4 mg **Measurement number: 4672**

Step	T[ºC]	^{39}Ar (%)[b]	^{40}Ar (mV)	rad (%)	$^{39}Ar/^{37}Ar$	$(^{36}Ar)_{Ca}$ (%)	$^{40}Ar^*/^{39}Ar$	error (± %)	age (Ma)	err. (± Ma)[c]
1	750	12.3%	2.52	70.3%	0.915	10.03%	1.73	3.45	41.2	1.40
2	850	8.6%	2.19	56.2%	0.287	13.13%	2.16	3.93	51.2	1.98
3[a]	970	37.8%	10.11	93.6%	0.102	84.44%	2.26	1.80	53.7	0.95
4[a]	995	10.2%	2.74	74.1%	0.067	58.00%	2.29	3.89	54.2	2.08
5[a]	1020	4.9%	1.35	62.9%	0.075	41.67%	2.31	4.92	54.9	2.66
6[a]	1150	6.8%	1.82	78.6%	0.069	63.86%	2.26	5.16	53.7	2.73
7[a]	1280	19.4%	5.00	63.5%	0.044	57.07%	2.19	2.33	52.0	1.20
							total gas age:		**51.7**	**4.80**
		cumulative ^{39}Ar defining plateau age:			**79.2%**		**plateau age:**		**53.4**	**5.09**

correcting factors Daly/HF = 8.35 ± 5.0% Ca 36/37 = 0.00024 K 40/39 = 0.0254

Ca 39/37 = 0.00039 J = 0.013352 ± 0.2%

a) steps used for calculating mean or plateau age c) 1σ error **constant correcting factors** $(^{40}Ar/^{36}Ar)_{air}$ = 299 ± 1.0 %

b) % of total ^{39}Ar released K/Ca-conv. = 0.247

Electronic supplement to: Ustaszewski K. et al., Tectonics, doi:10.1029/2010TC002668, 2010

Data Set S5: Electron-microprobe analyses of amphiboles dated by the $^{40}Ar/^{39}Ar$ stepwise heating technique. The analyses were performed by Jürgen Konzett on a JEOL microprobe at the Institute of Mineralogy & Petrography at the University Innsbruck.

Sample M120

	amph 1-1 rim	**amph 1-2 core**	**amph 2-1 rim**	**amph 2-2 core**	**amph 3-1 rim**	**amph 4-1 rim**	**amph 4-2 core**	**amph 5-1 rim**	**amph 5-2 core**	**amph 6 rim**
SiO2	45.24	49.46	45.40	51.87	44.68	47.45	55.99	45.44	51.82	45.50
TiO2	0.33	0.18	0.29	0.15	0.44	0.27	0.00	0.32	0.05	0.37
Al2O3	12.18	8.29	12.04	6.05	11.90	10.45	1.56	11.89	5.88	11.69
Cr2O3	0.07	0.00	0.07	0.06	0.00	0.14	0.00	0.05	0.00	0.05
Fe2O3	4.48	4.68	4.88	5.56	4.78	3.99	0.82	3.65	5.18	4.17
FeO	10.40	8.46	9.68	6.49	10.36	9.77	8.25	10.59	6.73	10.76
MnO	0.25	0.30	0.34	0.36	0.22	0.27	0.28	0.24	0.32	0.28
MgO	12.21	14.32	12.13	15.93	12.13	13.21	19.02	12.47	16.29	12.21
CaO	12.36	11.90	11.81	11.68	12.41	12.15	12.94	12.42	12.17	12.49
Na2O	1.75	1.24	1.85	1.05	1.61	1.51	0.25	1.79	0.98	1.55
K2O	0.32	0.37	0.32	0.32	0.34	0.44	0.05	0.32	0.27	0.35
H2O	2.08	2.11	2.08	2.14	2.07	2.1	2.17	2.08	2.14	2.08
Total	101.67	101.31	100.89	101.66	100.93	101.75	101.32	101.25	101.83	101.51
Si	6.507	7.023	6.558	7.265	6.485	6.766	7.791	6.555	7.254	6.560
Ti	0.036	0.019	0.032	0.016	0.048	0.029	0.000	0.035	0.005	0.040
Al	2.065	1.387	2.050	0.999	2.036	1.756	0.256	2.021	0.970	1.986
Cr	0.008	0.000	0.008	0.007	0.000	0.016	0.000	0.006	0.000	0.006
Fe3	0.485	0.500	0.531	0.586	0.522	0.429	0.086	0.396	0.546	0.453
Fe2	1.251	1.004	1.169	0.760	1.258	1.165	0.960	1.277	0.787	1.298
Mn	0.031	0.036	0.042	0.043	0.027	0.033	0.033	0.029	0.038	0.034
Mg	2.618	3.031	2.612	3.326	2.624	2.808	3.945	2.681	3.399	2.624
Ca	1.905	1.810	1.828	1.753	1.930	1.856	1.929	1.920	1.825	1.929
Na	0.488	0.341	0.518	0.285	0.453	0.418	0.067	0.501	0.266	0.433
K	0.059	0.067	0.059	0.057	0.063	0.080	0.009	0.059	0.048	0.064
Sum Cations	15.452	15.219	15.405	15.095	15.446	15.354	15.076	15.479	15.140	15.427
xMg (FeII+)	0.677	0.751	0.691	0.814	0.676	0.707	0.804	0.677	0.812	0.669
xMg (Fetot)	0.601	0.668	0.606	0.712	0.596	0.638	0.790	0.616	0.718	0.600
Fe3+/Fe(tot)	0.279	0.333	0.312	0.435	0.293	0.269	0.082	0.237	0.409	0.259
Al(IV)	1.493	0.977	1.442	0.735	1.515	1.234	0.209	1.445	0.746	1.441
Al(VI)	0.572	0.410	0.608	0.263	0.521	0.522	0.047	0.576	0.224	0.546
Na(M4)	0.095	0.190	0.172	0.247	0.070	0.144	0.000	0.080	0.175	0.071
Na(A)	0.393	0.152	0.346	0.038	0.383	0.274	0.067	0.420	0.091	0.362
Tschermaks	1.136	0.949	1.209	0.887	1.139	1.024	0.133	1.047	0.781	1.084
Cr - Al6	0.007	0.000	0.007	0.007	0.000	0.015	0.000	0.005	0.000	0.005
Fe3+ - Al6	0.426	0.528	0.439	0.660	0.458	0.418	0.647	0.378	0.699	0.418
Ti-vector	0.036	0.019	0.032	0.016	0.048	0.029	0.000	0.035	0.005	0.040
Edenite	0.452	0.219	0.405	0.095	0.446	0.354	0.076	0.479	0.140	0.427
Plagioclase	0.095	0.190	0.172	0.247	0.070	0.144	0.000	0.080	0.175	0.071
K - Na(A)	0.130	0.306	0.146	0.602	0.141	0.226	0.116	0.123	0.345	0.151
Fe2+ - Mg	0.321	0.247	0.306	0.184	0.322	0.291	0.194	0.320	0.186	0.328
Mn - Mg	0.008	0.009	0.011	0.010	0.007	0.008	0.007	0.007	0.009	0.009
FM - Ca (M4)	0.000	0.000	0.000	0.000	0.000	0.000	0.071	0.000	0.000	0.000

all analyses except amph 4-2 normalized to 13 cations + Na + K + Ca and 23 ox + stoichiometric (OH, F, Cl)
amph 4-2 normalized to 15 cations + Na + K and 23 ox + stoichiometric (OH, F, Cl)

cation allocation to lattice positions

Si	6.507	7.023	6.558	7.265	6.485	6.766	7.791	6.555	7.254	6.560
Al(IV)	1.493	0.978	1.442	0.735	1.515	1.234	0.209	1.445	0.746	1.441

Sample M120

	amph 1-1 rim	amph 1-2 core	amph 2-1 rim	amph 2-2 core	amph 3-1 rim	amph 4-1 rim	amph 4-2 core	amph 5-1 rim	amph 5-2 core	amph 6 rim
∑	8.000	8.000	8.000	8.000	8.000	8.000	8.000	8.000	8.000	8.000
Al(VI)	0.572	0.410	0.608	0.264	0.521	0.522	0.047	0.576	0.224	0.546
Ti	0.036	0.019	0.032	0.016	0.048	0.029	0.000	0.035	0.005	0.040
Cr	0.008	0.000	0.008	0.007	0.000	0.016	0.000	0.006	0.000	0.006
Fe3	0.485	0.500	0.531	0.586	0.522	0.429	0.086	0.396	0.546	0.453
Fe2	1.251	1.004	1.169	0.760	1.258	1.165	0.960	1.277	0.787	1.298
Mn	0.031	0.036	0.042	0.043	0.027	0.033	0.033	0.029	0.038	0.034
Mg	2.618	3.031	2.612	3.326	2.624	2.808	3.874	2.681	3.399	2.624
∑	5.000	5.000	5.000	5.000	5.000	5.000	5.000	5.000	5.000	5.000
Mg	0.000	0.000	0.000	0.000	0.000	0.000	0.071	0.000	0.000	0.000
Ca	1.905	1.810	1.828	1.753	1.930	1.856	1.929	1.920	1.825	1.929
Na	0.095	0.190	0.172	0.247	0.070	0.144	0.000	0.081	0.175	0.071
∑	2.000	2.000	2.000	2.000	2.000	2.000	2.000	2.000	2.000	2.000
Na	0.393	0.152	0.346	0.038	0.383	0.274	0.067	0.420	0.091	0.363
K	0.059	0.067	0.059	0.057	0.063	0.080	0.009	0.059	0.048	0.064
vac	0.548	0.781	0.595	0.905	0.554	0.646	0.924	0.521	0.861	0.573
∑	1.000	1.000	1.000	1.000	1.000	1.000	1.000	1.000	1.000	1.000

Sample M129

	Ca-Amphibole						FeMg-Amphibole	
	amph 1-1	amph 2-1	amph 3-1	amph 3-2	amph 5-1	amph 5-3	amph 1-2	amph 4
SiO2	48.81	48.53	44.55	50.66	48.44	43.96	53.41	52.74
TiO2	0.29	0.42	0.46	0.33	0.43	0.16	0.05	0.04
Al2O3	8.72	9.10	12.83	6.53	8.94	14.28	2.39	2.70
Cr2O3	0.00	0.00	0.13	0.09	0.00	0.00	0.00	0.00
Fe2O3	0.82	0.32	1.32	1.52	2.11	1.19	0.65	1.40
FeO	13.36	15.22	14.84	12.22	12.66	14.74	20.96	23.16
MnO	0.37	0.35	0.42	0.42	0.38	0.43	1.40	0.86
MgO	13.24	12.59	10.67	14.69	13.45	10.13	16.75	15.96
CaO	12.25	11.57	12.02	12.24	12.15	12.16	3.21	2.40
Na2O	1.08	1.12	1.65	0.84	1.05	1.69	0.31	0.30
K2O	0.14	0.08	0.23	0.06	0.13	0.24	0.00	0.00
H2O	2.08	2.08	2.05	2.11	2.10	2.05	2.08	2.07
Total	101.17	101.38	101.16	101.71	101.84	101.03	101.21	101.63
	normalized to 15 cations + Na + K and 23 oxygen + 2 (OH, F, Cl)							
Si	7.022	7.000	6.510	7.209	6.929	6.425	7.712	7.646
Ti	0.031	0.046	0.051	0.035	0.046	0.018	0.005	0.004
Al	1.479	1.547	2.210	1.095	1.507	2.460	0.407	0.461
Cr	0.000	0.000	0.015	0.010	0.000	0.000	0.000	0.000
Fe3	0.089	0.035	0.145	0.163	0.227	0.130	0.071	0.153
Fe2	1.608	1.836	1.813	1.455	1.514	1.802	2.532	2.808
Mn	0.045	0.043	0.052	0.051	0.046	0.053	0.171	0.106
Mg	2.839	2.707	2.324	3.116	2.868	2.207	3.605	3.449
Ca	1.888	1.788	1.882	1.866	1.862	1.904	0.497	0.373
Na	0.301	0.313	0.468	0.232	0.291	0.479	0.087	0.084
K	0.026	0.015	0.043	0.011	0.024	0.045	0.000	0.000
Sum Cations	15.327	15.328	15.51	15.243	15.315	15.524	15.087	15.084
xMg (FeII+)	0.638	0.596	0.562	0.682	0.654	0.550	0.587	0.551

Sample M129

	Ca-Amphibole						FeMg-Amphibole	
	amph 1-1	**amph 2-1**	**amph 3-1**	**amph 3-2**	**amph 5-1**	**amph 5-3**	**amph 1-2**	**amph 4**
xMg (Fetot)	0.626	0.591	0.543	0.658	0.622	0.533	0.581	0.538
Fe3+/Fe(tot)	0.052	0.019	0.074	0.101	0.131	0.067	0.027	0.052
Al(IV)	0.978	1.001	1.490	0.791	1.071	1.575	0.288	0.354
Al(VI)	0.500	0.546	0.719	0.304	0.436	0.885	0.119	0.108
Na(M4)	0.000	0.000	0.000	0.000	0.000	0.000	0.000	0.000
Na(A)	0.301	0.313	0.467	0.232	0.291	0.479	0.087	0.084
Tschermaks	0.651	0.673	0.980	0.548	0.756	1.051	0.201	0.269
Cr - Al6	0.000	0.000	0.015	0.018	0.000	0.000	0.000	0.000
Fe3+ - Al6	0.136	0.052	0.148	0.297	0.301	0.124	0.352	0.568
Ti-vector	0.031	0.046	0.051	0.035	0.046	0.018	0.005	0.004
Edenite	0.327	0.328	0.510	0.243	0.315	0.524	0.087	0.084
Plagioclase	0.000	0.000	0.000	0.000	0.000	0.000	0.000	0.000
K - Na(A)	0.079	0.045	0.084	0.045	0.075	0.085	0.000	0.000
Fe2+ - Mg	0.358	0.400	0.433	0.315	0.342	0.444	0.401	0.441
Mn - Mg	0.010	0.009	0.012	0.011	0.010	0.013	0.027	0.017
FM - Ca (M4)	0.112	0.212	0.118	0.134	0.138	0.096	1.503	1.627

cation allocation to lattice positions

Si	7.022	7.000	6.510	7.209	6.929	6.425	7.712	7.646
Al(IV)	0.978	1.001	1.490	0.791	1.071	1.575	0.288	0.354
∑	8.000	8.000	8.000	8.000	8.000	8.000	8.000	8.000
Al(VI)	0.500	0.546	0.719	0.304	0.436	0.885	0.119	0.108
Ti	0.031	0.046	0.051	0.035	0.046	0.018	0.005	0.004
Cr	0.000	0.000	0.015	0.010	0.000	0.000	0.000	0.000
Fe3	0.089	0.035	0.145	0.163	0.227	0.130	0.071	0.153
Fe2	1.608	1.836	1.813	1.455	1.514	1.802	2.532	2.808
Mn	0.045	0.043	0.052	0.051	0.046	0.053	0.171	0.106
Mg	2.727	2.494	2.206	2.982	2.730	2.111	2.102	1.822
∑	5.000	5.000	5.000	5.000	5.000	5.000	5.000	5.000
Mg	0.112	0.212	0.118	0.134	0.138	0.096	1.503	1.627
Ca	1.888	1.788	1.882	1.866	1.862	1.904	0.497	0.373
Na	0.000	0.000	0.000	0.000	0.000	0.000	0.000	0.000
∑	2.000	2.000	2.000	2.000	2.000	2.000	2.000	2.000
Na	0.301	0.313	0.468	0.232	0.291	0.479	0.087	0.084
K	0.026	0.015	0.043	0.011	0.024	0.045	0.000	0.000
vac	0.673	0.672	0.490	0.757	0.685	0.476	0.913	0.916
∑	1.000	1.000	1.000	1.000	1.000	1.000	1.000	1.000

Data Set S6: Summary of geochronological data from the Sava Zone used for constraining its thermal evolution. The data are separated into a footwall (*italics*) and hangingwall unit with respect to the Motajica detachment. All data except those indicated by superscripts were derived in this study. Compare with Figure 15 in the main manuscript.

sample	tectonic unit	lithology	method	age (Ma)	2σ error (Ma)	Tc (°C)	Tc err (°C)
			footwall units				
UK04-04	*M*	*granite*	*ap FT*	*15.2*	*2.2*	*85*	*25*
UK06-06	*M*	*granite*	*ap FT*	*16.5*	*2.4*	*85*	*25*
UK04-03	*M*	*granite*	*ap FT*	*14.7*	*1.6*	*85*	*25*
UK04-04	*M*	*granite*	*zr FT*	*16.7*	*2.4*	*250*	*50*
UK04-06	*M*	*granite*	*zr FT*	*16.3*	*2.2*	*250*	*50*
UK04-02	*P*	*orthogneiss*	*ap FT*	*16.8*	*2.4*	*85*	*25*
UK04-02	*P*	*orthogneiss*	*zr FT*	*21.0*	*2.0*	*250*	*50*
UK06-58	*P*	*Cc marble*	*Ar-Ar WM*	*25.0*	*1.5*	*350*	*25*
UK04-04	*M*	*granite*	*U-Pb Mz*	*26.6*	*0.2*	*725*	*50*
UK04-04	*M*	*granite*	*U-Pb Zr*	*26.7*	*0.0*	*900*	*50*
Pamic[1]	*M*	*granite*	*K-Ar Bi*	*18.1*	*0.6*	*300*	*20*
VIG-1[2]	*SD*	*metapelite*	*K-Ar Bi*	*32.5*	*11.0*	*300*	*20*
VIG-1[2]	*SD*	*metapelite*	*K-Ar Hbl*	*46.0*	*3.5*	*495*	*50*
M129	*M*	*amphibolite*	*Ar-Ar Hbl*	*53.4*	*5.1*	*495*	*50*
M120a	*M*	*amphibolite*	*Ar-Ar Hbl*	*58.5*	*6.0*	*495*	*50*
UK06-113[3]	*M*	*metapelite*	*EMPA Mz*	*61.0*	*15.0*	*585*	*90*
UK06-117[3]	*M*	*metapelite*	*EMPA Mz*	*59.0*	*13.0*	*585*	*90*
M121[3]	*M*	*metapelite*	*EMPA Mz*	*64.0*	*12.0*	*585*	*90*
			hangingwall units				
UK05-09	M	sandstone	ap FT	38.6	6.4	85	25
M107	M	sandstone	ap FT	27.1	4.2	85	25
M123	M	sandstone	ap FT	37.3	4.2	85	25
UK06-02	K	sandstone	ap FT	28.5	5.8	85	25
K149	K	dolerite	zr FT	56.4	6.8	250	50
K146	K	granite	zr FT	57.3	5.4	250	50
K150	K	rhyolite	zr FT	61.2	7.4	250	50
UK06-34	K	rhyolite	U-Pb Zr	81.6	0.1	900	50
K149	K	dolerite	U-Pb Zr	81.4	0.1	900	50

key:

K	Kozara
M	Motajica
P	Prosara
SD	Sava depression
Tc	closure temperature
Tc err	„error“ on the closure temperature; represents the range of closure temperatures around a „central“ value, defined in field Tc.

references:

1	Lanphere et al., 1988
2	Lanphere and Pamić, 1992
3	Krenn et al., 2008